SAND2018-9940J

Temperature Response of Soft Ionizable Polymer Nanoparticles

Sidath Wijesinghe, [1] Dvora Perahia[1*] and Gary S. Grest[2*]
[1]*Department of Chemistry, Clemson University, Clemson, South Carolina 29634, USA*
[2]*Sandia National Laboratories, Albuquerque, New Mexico 87185, USA*

Abstract

Temperature response of luminescent ionizable polymers confined into far from equilibrium nanoparticles without chemical links, was studied using molecular dynamics simulations. These nanoparticles often referred to as polydots, are emerging as a promising tool for nano medicine. Incorporating ionizable groups into these polymers enable bio functionality, however they also affect the delicate balance of interactions that hold these nanoparticles together. Here polydots formed by a model polymer dialkyl p-phenylene ethynylene (PPE), with varying number of carboxylate groups along the polymer backbone were probed. We find that increasing temperature results in a dynamic state that allows internal rearrangements of the polydots and migration of the ionizable groups towards the particle interface, while retaining the overall particle shape. The dependence of the transition temperature on the surface to volume ratio of these polydots is much stronger than what has previously been observed in polymeric thin films.

Sandia National Laboratories is a multimission laboratory managed and operated by National Technology & Engineering Solutions of Sandia, LLC, a wholly owned subsidiary of Honeywell International Inc., for the U.S. Department of Energy's National Nuclear Security Administration under contract DE-NA0003525.

I. INTRODUCTION

Soft nanoparticles (NPs) constitute a class of responsive structures for medical diagnostics and therapeutics.[1-5] Among them is a new class of NPs, or polydots, that consists of luminescent polymers confined into nano dimensions without additional chemical crosslinks.[5-11] These NPs are distinguished from traditional soft and hard NPs in their response to their environment that stems from their unique stability without crosslinks. These particles are highly emissive and their inherent photophysics is affected by the specific chemistries of the macromolecules, the polymer conformation, chain packing, and internal dynamics.[5-11] Confined into nano-dimensions, the polymer characteristics differ significantly from those of spontaneous aggregates. Polydots remain stable in water for extended time (months to years) and their internal dynamics is rather slow, consistent with a glassy state.[6, 7] Confined polymers have been thoroughly studied, predominantly focusing on the effects of tethering to surfaces (polymer brushes)[12] and the effects of interfaces on the glass transition temperature T_g of thin films.[13] There is however very limited understanding of confinement of macromolecules into nanoparticles where the volume to surface area becomes a critical factor, particularly in presence of ionizable groups. Our previous studies have established that in confinement of conjugated polymers into a nanoparticle leads to glassy behavior and introducing electrostatic interactions through ionizable groups affects both chain packing and dynamics at ambient temperatures.[7] Here we probe their response to thermal perturbation on the structure, dynamics and stability of ionizable polydots. This study shows that while the particles become more dynamic with increasing temperature, like their non-ionic analogues, concurrent rearrangements of the ionizable groups enhances stability.

While experimentally the photophysics of polydot has been intensively studied,[8] the first insight into their stability was obtained by Maskey et al.[6, 15] using molecular dynamics (MD) simulations. They studied confined dinonyl poly *para phenylene ethynylene* (PPE) as a model polymer. These are rigid luminescent polymers whose backbone consist of alternating single and triple bonds connecting aromatic rings.[16] As opposed to flexible and semi-flexible polymers, which collapse as the quality of the solvent is reduced, PPEs remain extended both in good and poor solvents.[17-19] They found that with increasing temperature alkyl substituted PPE polydots unravel and their shape becomes less spherical. The dynamics within the polydot was found to be highly constrained within the temperature range where the polymer remains confined.[6]

Introducing ionizable groups such as sulfonate, carboxylate and quaternary ammonium groups into polydots enable tailoring of functionality.[1, 20] However, ionizable groups also result in long range interactions, often beyond the size of the entire particle incorporating a strong force that is expected to affect the structure dynamics and stability of the polydots. With this realization, we have probed the structure and motion of polydots that consist of PPEs decorated by alkyl carboxylate chains, immersed in water, at ambient condition. [7] These studies have shown that in these ionizable polydots, the carboxylate groups tend to reside at the interface of the polydots. Furthermore, the presence of carboxylate groups affects the local dynamics of the polymer backbone, resulting in longer correlation times for aromatic rings tethered to carboxylate groups.[7] On the path to understand nano-confinement of polymers the current study probes for the first time the response of ionic decorated polydots to thermal stimuli. We show that temperature affects the internal dynamics and consequently, the distribution of the ionizable groups within the polydots and hence, impact the shape and stability of these soft NPs.

II. POLYDOT PREPARATION AND SIMULATION MODEL

Polydots are formed experientially by trapping the polymers in droplets of good solvent that is dripped into water. As the good solvent evaporates under sonication the polymers remain in a long lived trapped state.[9-11] Computationally, polydots were prepared in as closest possible way to the experimental procedure. [6, 15] To model the experimental process, an isolated PPE chain dissolved in a good solvent tetrahydrofuran (THF), was encapsulated in a spherical cavity where only the atoms of the PPE chain interact with the cavity wall by a purely repulsive harmonic potential. Good solvent evaporation is mimicked by decreasing the size of the confining cavity. Specifically, we compressed isolated dinonyl PPE chains with $(CH_2)_8CH_3$ and $(CH_2)_8COO^-$ side chains with n = 60, 120 and 240 monomers containing ~3960, 7930, and 15770 atoms respectively in a bath of 90 423 tetrahydrofuran (THF) molecules to obtain the polydots. The fraction of carboxylate group f is varied from 0 to 0.7 randomly by replacing the CH_3 end groups by carboxylate on one of the two side chains of each aromatic ring. f = 0 corresponds to the case in which all side chains are methyl terminated where f = 0.1, 0.2, 0.4 and 0.7 corresponds to polymers in which 10%, 20%, 40% and 70% of aromatic rings have one side chain terminated by a carboxylate group.[7] Charge neutrality is maintained by introducing one Na^+ counter ion for each carboxylate group. Once the collapsed PPE polydot density reaches its bulk value, the spherical cavity is removed and the polydots are transferred to water or run in an implicit poor solvent[22] with ε = 77.3 which mimics water. These implicit solvents offer the ability to study the behavior of larger polydots for longer times. For f=*0*, the polydots were studied in implicit poor solvents since it is computational too expensive to study the larger polydots in explicit solvent. Our previous studies for one molecular weight have shown that for f = 0 the radius of gyration of the polydot as

well as the radial density obtained in implicit solvents and in water are the same. [6, 15] All the ionic polydots ($f > 0$) were studied in water.

PPEs were modeled fully atomistically using the optimized potentials for liquid simulations-all atoms (OPLS-AA).[24, 25] Water is represented using the TIP4P/2005 water model[26, 27] and SHAKE algorithm is used to constrain the O-H bond length and H-O-H angle.[28, 29] While many properties including the equation of state and diffusion constant as function of temperature of TIP4P/2005 are in very good agreement with experiment, the dielectric constant of TIP4P/2005 water is lower than experiment.[29] Vega et al. found that the dielectric constant of TIP4P/2005 is $\varepsilon = 58$ at 298K compared to the experimental value of 78.[29,30]

All simulations were performed using the large-scale atomic/ molecular massively parallel simulator (LAMMPS)[31] molecular dynamics code. In THF and in water, all the Lennard-Jones 12:6 non-bonded interactions were truncated at a cutoff $r_c = 1.2$ nm. Coulomb interactions are treated with long-range particle−particle particle-mesh algorithm (PPPM)[32] Ewald with a real space cutoff of 1.2 nm and a precision of 10^{-4}. The quality of implicit solvents is controlled by varying the strength of the attractive interactions between non-bonded atoms. To model a poor solvent for both the backbone and side chains,[17] all Lenard Jones (LJ) nonbonded interactions are truncated at $r_c = 1.2$ nm.

To model polydots in water, we separately equilibrated a system of 121,604 water molecules with a spherical cavity located at the center of the simulation cell. This cavity is large enough to accommodate the polydot. At 300K, the polydot was placed in the center of the cavity and the system ran at constant pressure of P = 1 atm for 8 ns to remove the excess volume and then ran at constant volume. To study the thermal stability of the polydots, we increased the temperature T to 400K and ran the system at constant pressure P = 1 atm for 5 ns and then at constant volume.

A similar procedure was followed when we increased T to 500K, except that the constant pressure run was at P = 100 atm. The constant volume simulations ran for 200 to 250 ns depending on the system. In an implicit poor solvent, the simulations were run for a range of temperatures from 300 to 600 K. For all simulations a Langevin thermostat[33, 34] with a damping constant of 100 fs was used to regulate the temperature.

III. RESULTS

The thermal response of polydots with chains of length n = 60, 120 and 240 di-nonyl PPEs was studied for f = 0 in implicit poor solvent to elucidate the effects of molecular weights on the polydots and serve as a baseline for understanding the temperature-charge correlations in these soft nano-particles. The largest chain length studied corresponds to molecular weights where the

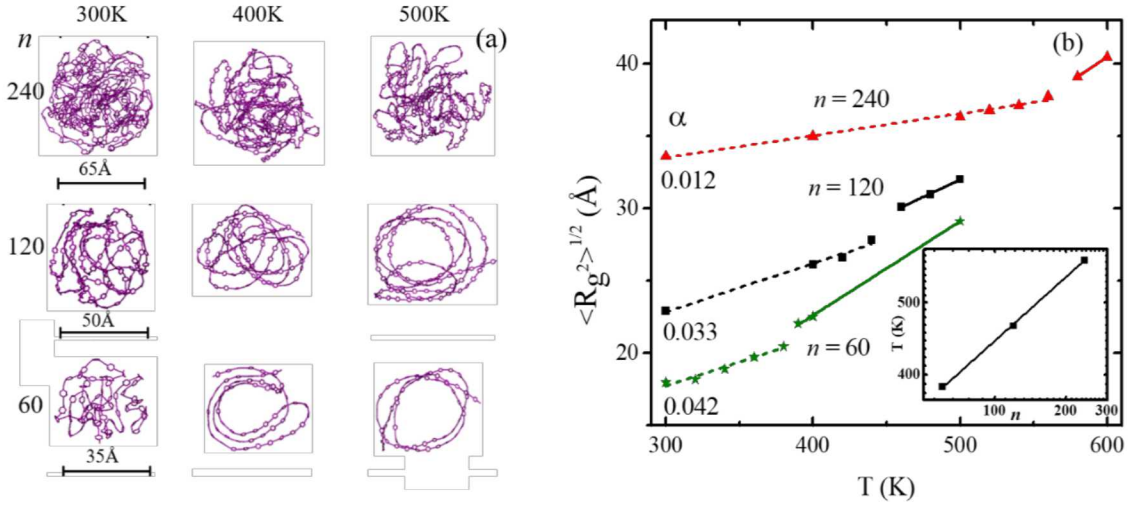

Figure 1-a) Polydots in an implicit poor solvent with ε= 77.3 at 200 ns at the indicated temperatures and n for f = 0. For clarity only, the backbone of the PPE chain is shown. b) Mean square radius of gyration $< R_g^2 >^{1/2}$ as a function of temperature for the indicated n. The slopes of the lines are denoted by α. *T*ransition temperature as a function of n is shown in inset.

polymer is soluble in organic solvents experimentally.[18, 19] The temperature range for the study is chosen below and above the glass transition temperature T_g of bulk PPEs.[18] Images of polydots at 200 ns in implicit poor solvent with ε = 77.3 are shown in Figure 1-a at different temperatures.

Upon increasing temperature, all polydots unravel, though the degree depends on the polymerization number. The n=60 and 120 polydots open whereas the larger n = 240 polydot expands, but retains its particulate shape up to 600K. The temperature response of the n = 240 polydot is similar to results obtained by Maskey et al[6] who showed that a n = 240 diethylhexyl PPE polydot (a polydot decorated with a different side chain) remained confined at 400K and partially opened up at 600K.

The average root mean squared radii of gyration $\langle R_g^2 \rangle^{1/2}$ of f = 0 polydots increases with increasing temperature as shown in Figure 1-b. A discontinuity in the slope of the line is observed as the polydots unravel, between 380K and 400 K for n = 60, between 440 K and 460 K for n= 120 and between 560 K and 580 K for n =240. Above these temperatures, $\langle R_g^2 \rangle^{1/2}$ increases faster with increasing T compared to lower temperatures. The rate of swelling with temperature is captured though the slope α, obtained from a linear fit of the lower T regime, shown in Figure 1-b. The rate of expansion decreases by a factor of ~ 3.5 as n increases from 60 to 240, indicative of the increasing thermal stability with increasing chain length. The transition temperature increases linearly with n as shown in the insert of Figure 1-b. This change takes place over a broad temperature window and is a signature of the unraveling of the polymer backbone. The transition appears to be similar in nature to T_g, where polymers become more dynamic and not a coil to globule transition since the transition is irreversible. While T_g is a bulk phenomenon, the term is borrowed here to describe the onset of dynamics. The time scale of dynamics as extracted from the autocorrelation function of the rotational motion of the aromatic rings at room temperature[7] clearly shows that the chains within the polydots are not crystalline. With increasing n, the surface to volume ratio of the polydot at low temperatures increases significantly affecting the onset of unraveling. Though the polydots studied here contain only one chain, this increase in the transition

temperature with decreasing surface to volume ratio is analogous with polymer thin films where T_g decreases as the surface to volume ratio increases.[13, 14]

The shape of polydots is one important parameter for their interaction with membranes however, it is rather challenging to capture small changes in symmetry of a dynamic nanoparticle. The ratios between the major three eigenvalues of moment of inertia tensor λ_i are used to follow these changes, where $\lambda_1 < \lambda_2 < \lambda_3$.[6, 7] The ratios of the two largest to the smallest eigenvalues λ_3/λ_1 and λ_2/λ_1 are able to capture the deviation from sphericity. For a sphere these ratios equal to 1.[6, 7]

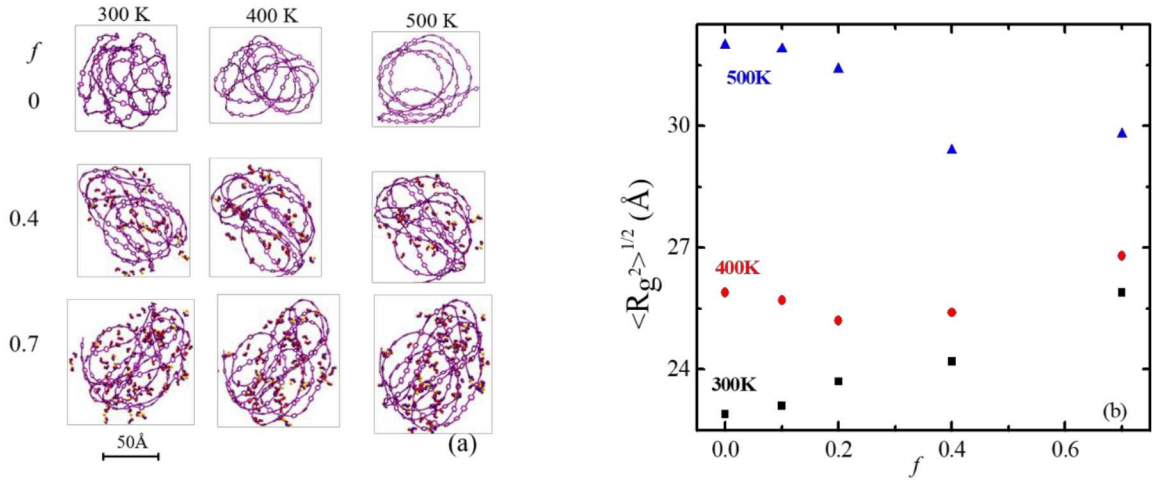

Figure 2-a) Polydots with n =120 in water at indicated temperatures in water f = 0.1, 0.4 and 0.7 after 180 ns. For clarity, only the backbone of the PPE chain is shown in purple. Carboxylate carbon is shown in blue, oxygen is in red and Na^+ counterion is shown in yellow. b) Mean square radius of gyration $<R_g^2>^{1/2}$ as a function of f for n =120 polydots at indicated temperatures in water.

Results for the 3 eigenvalues and their ratios for different n are summarized in Table S1. At 300K, λ_3/λ_1 = 1.3 and λ_2/λ_1 = 1.1 for n =60. For n = 240, λ_3/λ_1 = 1.5 and λ_2/λ_1 =1.3. These ratios are consistent with visual observation that the shaped polydot at room temperature and at low molecular weights slightly diverge from sphericity at room temperature. This deviation from sphericity increases with increasing M_w as well as temperature for all polydots studied.

Ionizable groups were then introduced into the polydots through terminating a fraction of the side chains with carboxylates that span the range from ionomers to polyelectrolytes.[35,36] These charged polydots were then studied as a function of temperature. These studies were carried out in water with the working assumption that the direct interaction of the solvent with the carboxylate groups constitutes one important factor in the thermal response of the ionizable polydots. The result for an intermediate polymerization number n = 120 polydots in water with f = 0.1, 0.4 and 0.7 are shown in Figure 2-a and the corresponding dimensions in Figure 2-b for three temperatures. Polydots in actual water constitute very large systems which are computationally expensive and therefore representative temperatures have been studied. Polydots with f = 0.1 and 0.2 unravel at 500K while those with f = 0.4 and 0.7 remain confined in the temperature range of this study. Enhanced stability is observed in the polyelectrolyte regime where in the ionomer region and the boundary between ionomers and polyelectrolytes, the behavior is similar to non-charged polydots. In non-charged PPEs within this temperature range, the polydots were not able to retain their particle state. The enhanced stability is a direct result of the ionizable groups.

The effects of temprature on the structure of the polydots in the different ionic regions was obtained by evaluating their symetry through the eigenvalues of the moment of inertia, calculating their scattering functions S(q) and their radial density. Yet again resolving changes within the small dimentions of the polydots that are critical to their stability and photophysics remains a challenge. The values of λ_3/λ_1 and λ_2/λ_1 along with $\langle R_g^2 \rangle^{1/2}$ of polydots with different f values are given in Table S2. $\langle R_g^2 \rangle^{1/2}$ is comparable in size for $f \leq 0.4$ and increase by 30-40% as T increases from 300K to 500K, while the polydot with most carboxylate groups, f = 0.7, is larger at 300K and increases slower as T increases. The ratio of the largest to smaller eigenvalue of radius of gyration tensor increases from 1.4 to 2.2 as T increases 300K to 500K for f = 0 compared to an increase of

1.8 to 2.3 from $f = 0.7$. These values suggest that even though the increasing temperature results in increasing the asphericity of polydots for all f values, the temperature dependent sphericity becomes less prominent for higher f. These results capture for the first time the competition between the inherent chain conformation and effects of confinement in the nano dimensions.

Further insight into structural changes of polydots as a function of temperatures was obtained by calculating the static form factor S(q), where q is the momentum transfer vector. It corresponds to the Fourier transform of the localized density. Results for the structure factor S(q) are shown in Figure S1. For $f = 0$, increasing T from 300 to 500 K results in a transformation from a sphere to an elliptical object with a hollow core. At 300 K, S(q) is well described by a fuzzy sphere form factor convoluted with a Gaussian to account for the finite interfacial width.[37] However, increasing T results in a transformation to ellipsoid shaped object at 400K and an oblate shaped object with a core at 500 K. For $f = 0.7$ an ellipsoid form factor captures the structure for all 3 temperatures, which is consistent with the results obtained through eigenvalues of the moment of inertia. The radius of gyrations extracted from S(q) are consistent with the calculated radii of gyration in Figure 2-b.

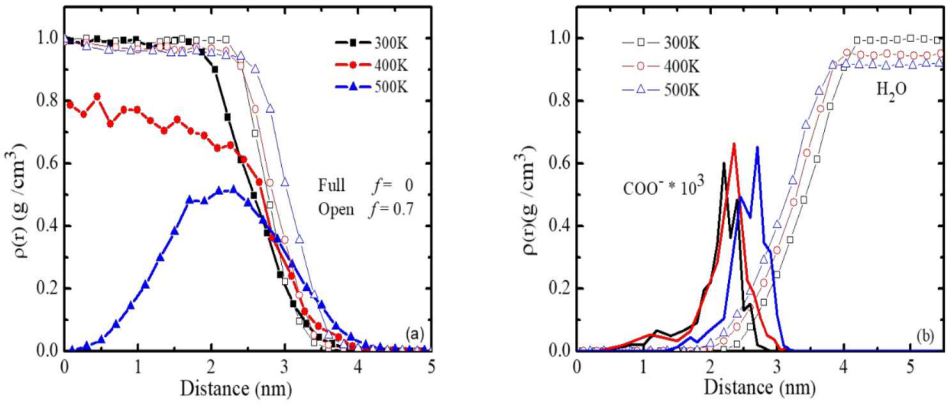

Figure-3 a) Radial mass density ρ(r) for the f = 0 (full) 0.7 (open) for entire polydot at indicated temperatures. b) Radial mass density for COO^- × 10^3 and water for f = 0.7 polydots at given temperatures.

Visualization has shown that with increasing temperature an internal cavity is formed for neutral and low f polydots where measurements of the eigenvalues of the moment of inertia and S(q) have shown a transformation in symmetry from spherical to elliptical, where the extent depends on f. The average radial mass density $\rho(r)$ of the polydots as a function of distance from their center of mass as the temperature is varied is shown in Figure 3 for f = 0 and 0.7. Following the density profiles of polymers and the carboxylate groups offers a unique insight into structural changes that take place within these far-from equilibrium soft nanoparticles. At 300K regardless of f, both polydots exhibit similar density profiles with a uniform density away from the interface, as shown in Figure 3-a. With increasing T, the density profile for f = 0 polydot first broadens at 400K and eventually develops a hollow center at 500K. This is in sharp contrast with the density profile for f = 0.7 polydots, which maintain similar shape over this temperature range.

The enhanced stability of these ionizable polydots and the shape changes observed with increasing temperature point towards potential changes in the distribution and clustering of the carboxylates. The radial mass density of carboxylates $\rho_{COO^-}(r)$ as a function of distance from polydot center of mass for f = 0.7 polydot for different T values along with the water density at the interface with the polydot are shown in Figure 3-b. At room temperature, a majority of the carboxylates reside at the polydot/water interface, as shown in our previous study.[7] Surprisingly, the clear maximum in $\rho_{COO^-}(r)$ near the polydot surface at room temperature, shifts towards the polydot/water interface as T increases. Specifically, at 300K for f = 0.7, 60 of the carboxylate groups at the polydot water interface while 24 carboxylate groups reside inside the polydot, while

at 500K, 72 carboxylate groups are at the polydot/water interface and only 12 carboxylate groups remain in the polydot interior. For all temperatures, the Na^+ counterions are condensed within the polydot. At the interface however, only about 50% of the Na^+ ions are condensed at 300K. The

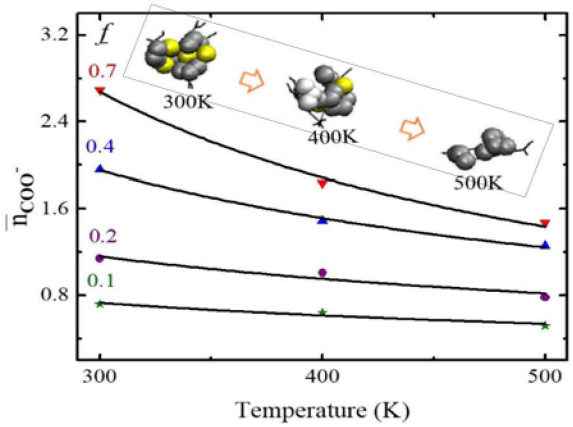

Figure 4: Average number of COO^- per ionic cluster in polydots with indicated *f* in water at given temperatures. Result are averaged over 2000 configurations. The inset shows the evolution of a representative ionic cluster in *f* = 0.7 polydot

fraction of condensed Na^+ atoms decreases to 30% at 500K. Here condensation is defined as being closer than 4Å from the center of mass of a carboxylate group. Increasing temperature enhances chain dynamics enabling rearrangements the carboxylates to phase segregate towards the water interface, shielding the predominantly hydrophobic polydot and enhancing the stability of this far-from-equilibrium NP.

The distribution of the carboxylate groups is one critical stability factor, particularly in the nano-dimensions where electrostatic interactions often exceed the dimensions of the clusters. At room temperature, the carboxylate groups within the polydots aggregate into ionic clusters and their formation is driven by the balance of electrostatic interactions and polydot backbone conformation.[7] As the Na^+ ions are fully condensed within the particle, the size of the ionic clusters within the polydots becomes an important stability parameter. The average number of COO^- groups residing in ionic clusters for different *f* as a function of temperature are presented in Figure

4. Two COO^- groups are defined to be in the same cluster if they are within 4 Å of each other. At 300K, increasing *f* from 0.1 to 0.7 results in an increase in the average cluster size from one or no clustering to 2.7. With increasing temperature, the large clusters break for all *f* as illustrated in Figure 4. However, for *f* = 0.4 and 0.7, the average cluster size remains larger than one. Combing clustering and excess hydrophilic later for polydots with a higher carboxylate fraction drive the enhanced stability of the polydots.

Increasing temperature has clearly shown enhanced dynamics where changes of dimensions with temperature capture the mesoscopic dynamics. Segmental dynamics particularly that of the aromatic rings in polymer backbone with respect to each other is one critical factor that impacts their glassy nature.[6, 37] The autocorrelation function $\langle N(t) \cdot N(0) \rangle$ of the aromatic rings, where *N(t)* is normal to their plane was calculated for polydots with different *f* values as the temperature is varied. The results for polydots with *f* = 0 and 0.7 at different temperatures are shown in Figure 5 for aromatic rings tethered to side chains terminated with CH_3 or COO^- groups.

Regardless of the temperature and *f*, the rings at the outer surface relax faster than the ones inside.

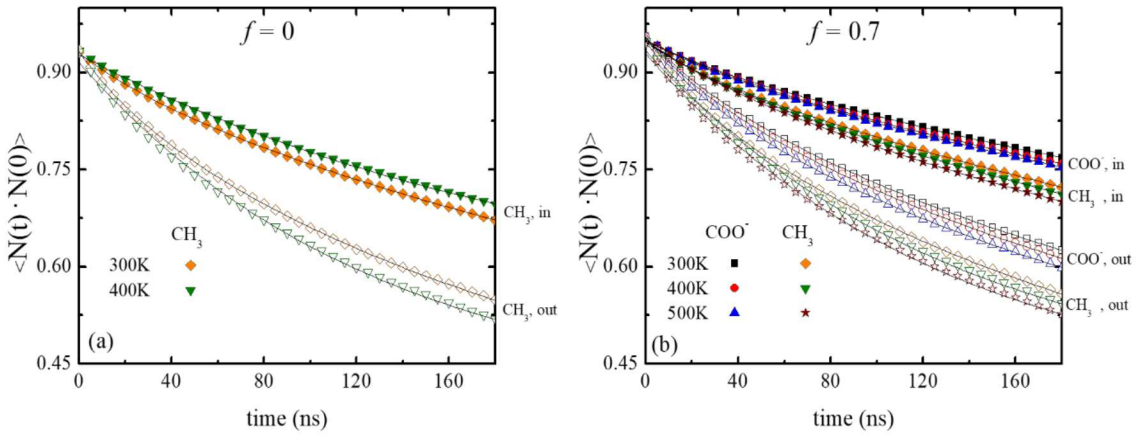

Figure: 5 Autocorrelation functions for aromatic rings in polydots with (a) $f = 0$ and (b) 0.7 connected to COO^- groups and CH_3 groups at indicated temperatures. Aromatic rings at the polydot interior (in) are shown in full symbols and rings at the outer surface (out) are shown in open symbols. The black lines correspond to KWW fits. The error bars on the fits are less than 1%.

The aromatic rings tethered to side chains terminated by COO^- groups relax slower than those terminated by CH_3 groups in all sites.

The correlation times for aromatic ring rotation were extracted by fitting the measured auto correlation function to the Kohlrausch−Williams−Watt (KWW)[38] function $\langle N(t)\cdot N(0)\rangle = A\exp(-t/\tau)^{\beta}$, where β is the stretched exponential and τ is the characteristic relaxation time. Results for τ are shown in Figure 6. The β values obtained from the fit are between 0.73 - 0.79 for all cases. The relaxation times τ for the aromatic rings are in the range of μs region for all temperatures. For all aromatic rings the relaxation time decreases with increasing temperature. The extent depends on the degree of interaction of the end group with the immediate surrounding. The increased correlation times for aromatic ring rotation at higher *f* is attributed to the trapping of the carboxylate groups into clusters as shown by Wijesinghe et al.[7] Overall, increasing temperature results in decreasing the ring correlation times for all *f* values as expected, due to the thermal energy. These results clearly show that through the ionizable groups enhance stability even for this small degree of clustering, thermal energy is sufficient to affect the dynamics.

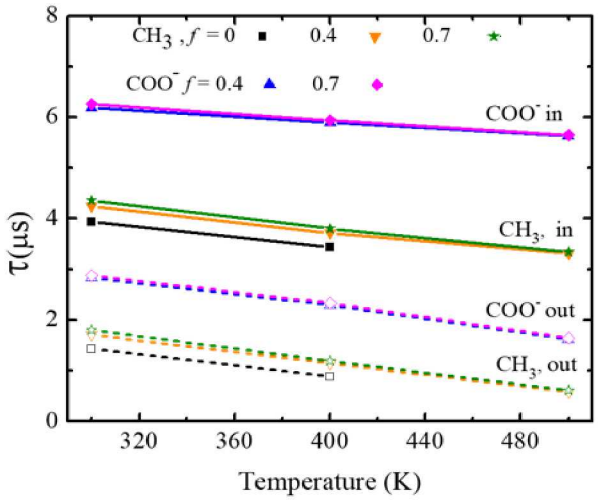

Figure 6: Correlation times for aromatic rings at the surface of the polydot and inside the polydot with indicated *f*, at given temperatures. Open symbols and dotted lines corresponds to the rings at the surface (out) full symbols and straight lines corresponds to the rings inside (in) of the polydot terminated with CH_3 with COO^- groups.

Finally, we probe the polydot-water interface whose hydrophobicity is decreased as more carboxylate groups migrate to the interface with increasing temperature. The residence time of water molecules near the carboxylate groups were calculated along with residence time of water molecules at the polydot surface for $f = 0$. [39, 40] The residence time of water molecules was calculated by identifying which of the water molecules reside within 3 Å of a carboxylate group for $f > 0$, or the polydot surface for $f = 0$. These water molecules were followed in time, determining when they moved out of this region. The data are normalized by the average number of water molecules that reside within the cut-off distance over the length of the run. For comparison we calculated the residence time of two water molecules far from the polydot. The results for $f = 0$, 0.4 ad 0.7 polydots are shown in Figure 7.

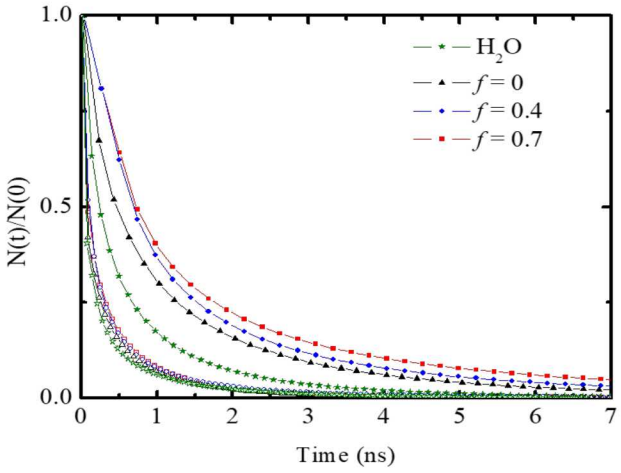

Figure 7: Residence time of water at a cutoff distance of 3 Å. The data are normalized by the average number of water molecules that reside within the cutoff distance. Full symbols represent residence time at 300K, open symbols represent the residence time at 500K for indicated system.

The residence time dynamics can be approximated by a single exponential function[40] $N(t) / N(0) = Ae^{-\frac{t}{t_r}}$ where, t_r is the mean residence time of water molecules at the polydot surface. The results for t_r are summarized in Table 1. At 300K, t_r = 0.52 ns for two water molecules far from the polydot, 0.98 ns for $f = 0$ polydot, 1.12ns for $f = 0.4$ polydot and 1.30 ns

for $f = 0.7$ polydot in water. At 500K however the residence times become shorter with $t_r = 0.03$ ns for bulk water, 0.05 ns for $f = 0$ polydot, 0.06 ns for $f = 0.4$ polydot and 0.08 ns for $f = 0.7$ polydot.

	t_r (ns) at 300K	t_r (ns) at 500K
Bulk water	0.52	0.03
$f = 0$	0.98	0.05
$f = 0.4$	1.12	0.06
$f = 0.7$	1.30	0.08

Table 1: Mean residence times t_r for water molecules at the polydot surface for a cut off distance of 3Å. Error bars for the fit to a exponential are 2%.

At both temperatures, the residence time for a water molecule near the polydot surface are longer to the residence time of two water molecules far away from the polydot surface. Increasing temperature results in decreasing the residence time of water molecules. The water molecules reside slightly longer near polydots with $f = 0.4$ and 0.7 compared to $f = 0$, independent of temperature. This is consistent with the relaxation times measured for the carboxylate groups at the interface as discussed in Figure 6.

IV. CONCLUSIONS

This study has provided a first ever temperature-charge correlation in polydots. Similar to their neutral analogues, ionizable polydots are far-from equilibrium soft nanoparticles that remain confined without crosslinks. However, in contrast to their neutral analogues that lose their particle nature, thermal energy induces dynamics that enable segregation of the ionizable groups to the interfacial region, hence changing their nature, while retaining their particulate state. The structure and shape evolution of the polydots with increasing temperature were initially visualized revealing that the nanoparticles become dynamic, through depending on the degree of decoration with ionizable group either unravel or remain in their collapsed state. Several means were employed to

capture changes within such small disordered particles. The changes in the overall symmetry of the polydots were captured by calculating the ratios of the eigenvalues of the moment of inertia, followed by measurements of the structure factor to attain the structure. Finally, measurements of the radial density to reveal internal rearrangements were carried out. Regardless of the polymerization number and the fraction of ionizable groups, all polydots expand with increasing temperature accompanied by a shape transformation into more elliptical NPs.

The backbone dynamics was probed through calculations of the autocorrelation function of the aromatic rings. For non-ionic polydots a transition from a glass like particle to a more dynamic state takes place with a strong dependence on chain length. For ionic polymers, small ionic clusters that decrease in size with increasing temperature are observed within the polydots. The system becomes sufficiently dynamic to allow migration of trapped carboxylate groups into the water interface.

The response of the ionizable polydots is thus two folds: while the dynamics increases with temperature driving the system to swell, the hydrophilic groups migrate to the interface forming a lower energy interface with water and enhance stability. Further, these results obtained for a single chain polydots have shown that within the small volume of a polydot ionic clustering takes place and is affected by temperature. The role of these ionic clusters in determining shape and stability remains an open question. Studies of multiple chain polydots are currently on the way to understand the effects of entropy and chain orientation on the structure and dynamics of polydots.

SUPPLEMENTARY MATERIAL

See supplementary material for a figure illustrating the procedure for making the polydots and a figure for the static structure factor S(q) for $f = 0.0$ and 0.7. Table with three eigenvalues (λ_1, λ_2,

λ_3) of radius of gyration tensor and their ratios for $f = 0.0$ in implicit solvent and $f = 0$ - 0.7 in water for $T = 300$, 400 and 500K.

ACKNOWLEDGEMENT

DP kindly acknowledged NSF DMR 1611136 for partial support. This work was performed, in part, at the Center for Integrated Nanotechnologies, an Office of Science User Facility operated for the U.S. Department of Energy (DOE) Office of Science. Sandia National Laboratories is a multi-mission laboratory managed and operated by National Technology and Engineering Solutions of Sandia, LLC, a wholly owned subsidiary of Honeywell International, Inc., for the U.S. Department of Energy's National Nuclear Security Administration under Contract DE-NA0003525. This paper describes objective technical results and analysis. Any subjective views or opinions that might be expressed in the paper do not necessarily represent the views of the U.S. Department of Energy or the United States Government.

* Corresponding Authors: D. Perahia (dperahi@g.clemson.edu) and G. S. Grest (gsgrest@sandia.gov)

References

1. L. Feng, J. Zhu and Z. Wang, *ACS Applied Materials Interfaces* **8**, 19364 (2016).

2. X. Feng, F. Lv, L. Liu, H. Tang, C. Xing, Q. Yang and S. Wang, *ACS Applied Mater/ Interfaces* **2**, 2429 (2010).

3. L. Feng, C. Zhu, H. Yuan, L. Liu, F. Lv and S. Wang, *Chem. Soc. Rev.* **42**, 6620 (2013).

4. X. Feng, L. Liu, S. Wang and D. Zhu, *Chem. Soc. Rev.* **39**, 2411 (2010)

5. E. Ahmed, S. W. Morton, P. T. Hammond and T. M. Swager, *Adv Mater*. **25**, 4504 (2013)

6. S. Maskey, N. C. Osti, G. S. Grest and D. Perahia, *Macromolecules* **49**, 2399 (2016).

7. S. Wijesinghe, S. Maskey, D. Perahia and G. S. Grest, *J. Chem. Phys.* **146**, 244907 (2017).

8. Y. Jiang and J. McNeill, *Chem. Rev.* **117,** 838 (2017).

9. Z. Tian, J. Yu, C. Wu, C. Szymanski and J. McNeill, *Nanoscale.* **2**, 1999 (2010).

10. C. Wu, C. Szymanski, Z. Cain and J. McNeill, *J. Am. Chem. Soc.* **129**, 12904 (2007).

11. C. Wu, B. Bull, C. Szymanski, K. Christensen and J. McNeill, *ACS Nano.* **2**, 2415 (2008).

12. J. Rühe, M. Ballauff, M. Biesalski, P. Dziezok, F. Gröhn, D. Johannsmann, N. Houbenov, N. Hugenberg, R. Konradi, S. Minko and M. Motornov, *Adv. Polym. Sci*. **165**, 79 (2004).

13. J. Forrest, K. DalnokiVeress, J. Stevens and J. Dutcher, *Phys. Rev. Lett.* 77, 2002 (1996).

14. C. J. Ellison and J. M. Torkelson, *Nature Materials* **2**, 695 (2003).

15. S. Maskey, N. C. Osti, D. Perahia and G. S. Grest, *ACS Macro Lett.* **2**, 700 (2013).

16. U. H. F. Bunz, *Macro. Rapid Comm.* **30**, 772 (2009).

17. S. Wijesinghe, S. Maskey, D. Perahia and G. S. Grest, *J. Polymer Science Part B-Polymer Phys.* **54**, 582 (2016).

18. D. Perahia, R. Traiphol and U.H. F. Bunz, *Macromolecules* **34**, 151 (2001).

19. D. Perahia, R. Traiphol and U. H. F. Bunz, *J. Chem. Phys.* **117**, 1827 (2002).

20. L. Zhou, J. Geng, G. Wang, J. Liu and B. Liu, *Polymer Chem.* **20**, 5243 (2013).

21. A. Agrawal, D. Perahia and G. S. Grest, *Phys. Rev. Lett.* **116**, 158001 (2016).

22. A. Agrawal, D. Perahia and G. S. Grest, *Phys. Rev. E 9***2**, 022601 (2015).

23. G. S. Grest and M. Murat, *Macromolecules* **26**, 3108 (1993).

24. W. Jorgensen, D. Maxwell and J. TiradoRives, *J. Am. Chem. Soc.* **118**, 11225 (1996).

25. W. Jorgensen, J. Madura and C. Swenson, *J. Am. Chem. Soc.* **106**, 6638 (1984).

26. J. L. Abascal and C. Vega, *J. Chem. Phys.* **123**, 234505 (2005).

27. C. Vega, J. L. Abascal, M. Conde and J. Aragones, *Faraday dDiscussions.* **141**, 251 (2009).

27. C. Malmberg and A. Maryott, *Res Nat Bureau Stand.* **56**, 1 (1956).

29. H. C. Andersen, *J. Computational Physics.* **1**, 24 (1983).

30. J. P. Ryckaert, G. Ciccotti and H. J. C. Berendsen, *J. Comp. Phys.* **23**, 327 (1977).

31. S. Plimpton, *J. Computational Physics.* **117**, 1 (1995).

32. R. W. Hockney and J. W. Eastwood (Adam Hilger-IOP, Bristol, 1988).

33. T. Schneider and E. Stoll, *Phys. Rev. B* **13**, 1302 (1978).

34. G. S. Grest and K. Kremer, *Phys. Rev. A* **33**, 3628 (1986).

35. A. Dobrynin and M. Rubinstein, *Prog. Polymer Science.* **30**, 1049 (2005).

36. H. Jiang, P. Taranekar, J. R. Reynolds and K.S. Schanze, *Angewandte Chemie-International Edition.* **48**, 4300 (2009).

37. D. J. Plazek and K. L. Ngai, *Macromolecules* **24**, 1222 (1991).

38. G. Williams and D. Watts, *Trans. Faraday Society.* **66**, 80 (1970).

39. S. Maskey, F. Pierce, D. Perahia and G. S. Grest, *J. Chem. Phys.* **134**, 244906 (2011).

40. Y. He, Y. Chang, J. C. Hower, J. Zheng and S. Chen, *Physical Chemistry Chemical Physics.* **36**, 5539 (2008).